Int. J. Heat Mass Transfer. Vol. 14, pp. 1705–1716. Pergamon Press 1971. Printed in Great Britain

TURBULENT HEAT AND MASS TRANSFER BETWEEN WALL AND FLUID STREAMS OF LARGE PRANDTL AND SCHMIDT NUMBERS

T. MIZUSHINA, F. OGINO, Y. OKA and H. FUKUDA
Department of Chemical Engineering, Kyoto University, Kyoto, Japan

(*Received* 30 *June* 1970)

Abstract—The expression for eddy diffusivity in a previous analysis was revised. By using the revised expression, good agreement was obtained between the predicted and experimental results for mass transfer at Schmidt numbers between 800 and 15,000.

Both the predicted and experimental results showed that the Sherwood number varies with $\frac{1}{3}$ power of the Schmidt number and about 0·9 power of the Reynolds number at Sc = 800–15,000 and Re = 3000–80,000.

NOMENCLATURE

- A, coefficient in equation (28);
- C_p, heat capacity [cal/g°C];
- c, concentration [g-mole/cm^3];
- c^*, dimensionless concentration $= (c - c_w)/(c_b - c_w)$;
- D, molecular diffusivity for mass [cm^2/s];
- d, diameter of eddy particle [cm];
- F, Faraday constant [coulomb/g-mole];
- f, friction factor;
- H, half width of two-dimensional channel [cm];
- H^+, dimensionless half width of two-dimensional channel $= Hu^*/\nu$;
- h, heat transfer coefficient [cal/cm^{2}s°C];
- h^+, dimensionless heat transfer coefficient $= h/\rho C_p u_*$;
- i, limiting current density [A/cm^2];
- K, mass transfer coefficient [cm/s];
- K^+, dimensionless mass transfer coefficient $= K/u_*$;
- k, constant in equation (13b);
- L^+, dimensionless entry length of mass transfer $= Lu_*/\nu$;
- l, mixing length [cm];
- Nu, Nusselt number;
- n, exponent in equation (18);
- Pr, Prandtl number;
- Re, Reynolds number;
- Sc, Schmidt number;
- Sh, Sherwood number;
- T, temperature [°C];
- T^*, dimensionless temperature $= (T - T_w)/(T_b - T_w)$;
- U, time-smoothed velocity in x-direction [cm/s];
- u, intensity of fluctuating velocity in x-direction [cm/s];
- u_*, friction velocity [cm/s];
- v, intensity of fluctuating velocity in y-direction [cm/s];
- x, distance in the flow direction [cm];
- y, distance perpendicular to the wall [cm];
- y^+, dimensionless distance from the wall $= yu_*/\nu$;
- $y_1{}^+$, boundary between the region where equation (28) is valid and that where equation (29) is valid;
- $y_2{}^+$, boundary between the region where equation (29) is valid and that where equation (30) is valid;
- $y_B{}^+$, boundary between the region where equation (34) is valid and that where equation (35) is valid;

y_H^+, boundary between the region where equation (31) is valid and that where equation (32) is valid.

Greek symbols

α, molecular diffusivity for heat [cm^2/s];
δ^+, dimensionless thickness of boundary layer;
ε_D, eddy diffusivity for mass [cm^2/s];
ε_H, eddy diffusivity for heat [cm^2/s];
ε_M, eddy diffusivity for momentum [cm^2/s];
η_H, equation (14a);
η_M, equation (13a);
$\kappa, \kappa_1, \kappa_2$, constants;
ν, kinematic viscosity [cm^2/s];
ρ, density [g/cm^3];
σ, $\varepsilon_H/\varepsilon_M$;
ϕ_H, equation (14b);
ϕ_M, equation (13b).

Subscripts

b, bulk;
w, wall.

INTRODUCTION

NUMEROUS equations have been proposed for predicting the heat or mass transfer rates between a pipe wall and a fully developed turbulent flow. Most of them are adequate only for Prandtl or Schmidt numbers of unity or less. Their inadequacy at large Prandtl and Schmidt numbers is principally caused by the expressions used for the eddy diffusivity in the region very close to the wall. This region is important because of the extremely large temperature or concentration gradients at large Prandtl or Schmidt numbers.

Regarding the eddy diffusivity in this region, the semiempirical relationships of Lin *et al.* [1] and of Deissler [2] are well-known, but their resulting equations for the heat or mass transfer rates differ in the predicted effect of the Prandtl or Schmidt number on the transfer rate. The equation of Lin *et al.* predicts that at large Prandtl or Schmidt numbers the Nusselt or Sherwood number varies with $Pr^{\frac{1}{3}}$ or $Sc^{\frac{1}{3}}$, while Deissler's equation leads to an exponent of $\frac{1}{4}$.

Measurements of heat or mass transfer rates have been made by many investigators at large Prandtl or Schmidt numbers, but most of their experimental results are too scattered and different from each other to determine the effect of the Prandtl or Schmidt number on the transfer rates.

Recently Mizushina *et al.* [3] measured the eddy diffusivities for heat using a Mach–Zehnder interferometer at $Pr = 6$–40 and also presented [4] an analytical expression for the ratio of the eddy diffusivities for heat and momentum transfer by modifying the mixing length theory.

This paper reports the comparison between the mass transfer rates obtained experimentally and those predicted by using the revised expression of the previous analysis for the eddy diffusivity, and discusses the effect of the Prandtl and Schmidt number on the heat and mass transfer coefficients respectively.

ANALYSIS

For a steady, fully developed rectilinear flow between parallel plates, the time-smoothed temperature and concentration equations may be written as

$$U\frac{\partial T}{\partial x} = \frac{\partial}{\partial y}\left[(\alpha + \varepsilon_H)\frac{\partial T}{\partial y}\right] \tag{1}$$

$$U\frac{\partial c}{\partial x} = \frac{\partial}{\partial y}\left[(D + \varepsilon_D)\frac{\partial c}{\partial y}\right]. \tag{2}$$

It may be assumed that the convection terms on the left sides of equations (1) and (2) can be neglected; in other words, the heat or mass flux is assumed to be constant at any value of y. This assumption may not cause serious errors at large Prandtl or Schmidt numbers because the temperature or concentration gradients are unimportant in the region far from the wall.

With this assumption, equations (1) and (2) may be rewritten in dimensionless form as

$$0 = \frac{\mathrm{d}}{\mathrm{d}y^+}\left[\left(\frac{1}{Pr} + \frac{\varepsilon_H}{\nu}\right)\frac{\mathrm{d}T^*}{\mathrm{d}y^+}\right] \tag{3}$$

$$0 = \frac{\mathrm{d}}{\mathrm{d}y^+}\left[\left(\frac{1}{Sc} + \frac{\varepsilon_D}{\nu}\right)\frac{\mathrm{d}c^*}{\mathrm{d}y^+}\right]. \tag{4}$$

Boundary conditions are

$$T^* = 0, c^* = 0 \quad \text{at} \quad y^+ = 0 \tag{5}$$

$$T^* = 1, c^* = 1 \quad \text{at} \quad y^+ = \infty \tag{6}$$

The values of T^* and c^* at $y^+ = \infty$ are essentially unity because both temperature and concentration are very nearly constant except in the region very close to the wall, and they are considered to be the bulk temperature or concentration at large Prandtl or Schmidt numbers.

Equations (3) and (4) are integrated, with the boundary conditions (5) and (6), to be

$$T^* = \int_0^{y^+} \frac{\mathrm{d}y^+}{1/Pr + \varepsilon_H/\nu} \Bigg/ \int_0^{\infty} \frac{\mathrm{d}y^+}{1/Pr + \varepsilon_H/\nu} \tag{7}$$

$$c^* = \int_0^{y^+} \frac{\mathrm{d}y^+}{1/Sc + \varepsilon_D/\nu} \Bigg/ \int_0^{\infty} \frac{\mathrm{d}y^+}{1/Sc + \varepsilon_D/\nu}. \tag{8}$$

It can be shown from the definitions of the heat and mass transfer coefficients that

$$h^+ = 1 \Bigg/ \int_0^{\infty} \frac{\mathrm{d}y^+}{1/Pr + \varepsilon_H/\nu} \tag{9}$$

$$K^+ = 1 \Bigg/ \int_0^{\infty} \frac{\mathrm{d}y^+}{1/Sc + \varepsilon_D/\nu} \tag{10}$$

and the Nusselt number and Sherwood number are given by

$$Nu = Re\sqrt{f/2} \quad Pr\, h^+ \tag{11}$$

$$Sh = Re\sqrt{f/2} \quad Sc\, K^+ \tag{12}$$

Expressions for eddy diffusivity

To evaluate the Nusselt and Sherwood numbers, the eddy diffusivities ε_H and ε_D must be evaluated over a cross section of the flow.

Mizushina *et al.* [4] proposed an expression for eddy diffusivity for heat by using their experimental results of ε_H/ν.

The basic concept of their theory is that a spherical eddy particle loses a part of its heat and momentum as it travels over a distance equal to the mixing length.

Assuming Newton's law for the drag force on an eddy particle, one obtains the following equations:

$$\varepsilon_M/\nu = \eta_M(lv/\nu) \tag{13}$$

where

$$\eta_M = \frac{\exp(2\phi_M) - 1}{\exp(2\phi_M) + 1} \cdot \frac{1}{\phi_M} \tag{13a}$$

$$\phi_M = \left(k \frac{l}{d} \frac{u}{v} \frac{1}{\eta_M}\right)^{\frac{1}{2}}. \tag{13b}$$

If the relation of Ranz and Marshall [5] is assumed to apply to the heat transfer from an eddy particle to the surroundings, the following expressions are obtained.

$$\varepsilon_H/\nu = \eta_H(lv/\nu) \tag{14}$$

where

$$\eta_H = \phi_H[1 - \exp(-1/\phi_H)] \tag{14a}$$

$$\phi_H = \frac{(d/l)^2 (1/\eta_M)(\varepsilon_M/\nu) Pr}{12 + 3{\cdot}6\sqrt{[(d/l)(1/\eta_M)(\varepsilon_M/\nu)]}\, Pr^{\frac{1}{3}}} \tag{14b}$$

Thus, to evaluate the eddy diffusivity for heat, the functional forms or values of l/d, η_M and ε_M/ν are required.

Assumption for l/d. The value of the mixing length is assumed to be determined by quantities that have local characters of turbulence, such as the diameter of the eddy particle, d, and the local Reynolds number of turbulence, dv/ν.

Thus,

$$l/d = fn(dv/\nu). \tag{15}$$

If the diameter of the eddy particles is considered to be the micro scale of turbulence, equation

(15) represents the same assumption as that of von Kármán [6].

Moreover, it may be reasonable to consider that $\partial u/\partial x \approx u/d$ and $\partial v/\partial y \approx v/l$. From the continuity equation, one obtains

$$l/d \approx v/u. \tag{16}$$

Substitution of equation (16) into equation (13b) gives the result that η_M is a constant.

Therefore, from equations (13) and (15), l/d may be considered to have the following functionality.

$$l/d = Fn\,(\varepsilon_M/\nu). \tag{17}$$

The simplest form is

$$l/d = \kappa\,(\varepsilon_M/\nu)^{1/n}. \tag{18}$$

Substitution of equation (18) into equation (14b) gives the result,

$$\phi_H = \frac{(1/\kappa^2\eta_M)\,(\varepsilon_M/\nu)^{1-(2/n)}\,Pr}{12 + 3{\cdot}6\sqrt{(1/\kappa\eta_M)\,(\varepsilon_M/\nu)^{(n-1)/2n}\,Pr^{\frac{1}{2}}}}. \tag{19}$$

Determination of the values of η_M *and* n. In the turbulent core, it may be assumed that $u \approx v$, and one obtains $l/d \approx$ constant in the order of unity from equation (16), i.e. the power number $1/n$ in equation (18) is zero.

Equation (19) is rewritten as

$$\phi_H = \frac{(1/\kappa_1{}^2\eta_M)\,(\varepsilon_M/\nu)\;Pr}{12 + 3{\cdot}6\sqrt{(1/\kappa_1\eta_M)\,(\varepsilon_M/\nu)^{\frac{1}{2}}\,Pr^{\frac{1}{2}}}}. \tag{20}$$

From equations (13) and (14), the ratio of eddy diffusivities for heat and momentum is

$$\sigma = \varepsilon_H/\varepsilon_M = \eta_H/\eta_M. \tag{21}$$

As seen from equations (14a) and (20), the value of η_H approaches unity when ε_M/ν increases to infinity, and η_M is a constant. Hence one obtains

$$\lim_{\varepsilon_M/\nu \to \infty} \sigma = 1/\eta_M. \tag{22}$$

From the experimental results of Mizushina *et al.* [7] for the ratio of the eddy diffusivities in the turbulent core region at large Prandtl numbers, the value of $\lim \sigma$ is supposed to be unity, so the value of η_M is taken to be unity. The following expression for the ratio of the eddy diffusivities is obtained from equations (14a) and (21) with $\eta_M = 1$:

$$\sigma = \phi_H\,[1 - \exp\,(-1/\phi_H)]. \tag{23}$$

The function ϕ_H in the turbulent core is given by equation (20) with $\eta_M = 1$.

In the vicinity of the wall, u and v are considered to be proportional to the distance from the wall and to the square of the distance, respectively. Hence from equation (16), one obtains

$$l/d \propto y. \tag{24}$$

By comparing equation (24) with equation (18), one obtains the following expression for the eddy diffusivity of momentum near the wall.

$$\varepsilon_M/\nu \propto (y)^n. \tag{25}$$

In this region, equation (23) is simplified to $\sigma \doteqdot \phi_H$, and using equation (25) and the simplified form of equation (19), one obtains

$$\varepsilon_H/\nu \doteqdot (Pr/12\kappa^2)\,(\varepsilon_M/\nu)^{2-(2/n)} \propto y^{2n-2}. \tag{26}$$

The experimental results of Mizushina *et al.* [3] for the eddy diffusivities of heat in the region near the wall shows that $\varepsilon_H/\nu \propto (y)^4$, and hence by comparing with equation (26) one obtains the result that the value of n is 3.

Thus, in the region close to the wall,

$$\phi_H = \frac{(1/\kappa_2{}^2)\,(\varepsilon_M/\nu)^{\frac{1}{3}}\,Pr}{12 + 3{\cdot}6\sqrt{(1/\kappa_2)\,(\varepsilon_M/\nu)^{\frac{1}{3}}\,Pr^{\frac{1}{2}}}}. \tag{27}$$

Eddy diffusivity for momentum. Mizushina *et al.* [8] have presented simple and systematic expressions for the eddy diffusivity for momentum as follows;

$$0 \leqq y^+ \leqq y_1{}^+ \qquad \varepsilon_M/\nu = A\,(y^+)^3 \tag{28}$$

$$y_1{}^+ \leqq y^+ \leqq y_2{}^+ \qquad \varepsilon_M/\nu = 0{\cdot}4\,y^+ (1 - y^+/H^+) - 1 \tag{29}$$

$$y_2{}^+ \leqq y^+ \leqq H^+ \qquad \varepsilon_M/\nu = 0{\cdot}07\,H^+. \tag{30}$$

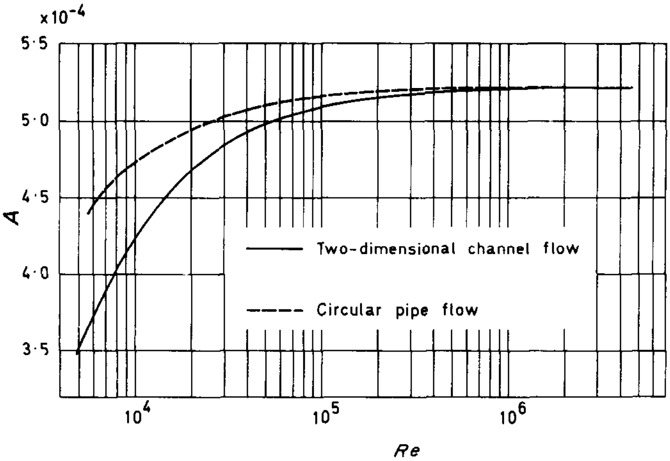

FIG. 1. Variation of the coefficient A with Reynolds number.

The values of A are depicted in Fig. 1 which shows that the value of A, and hence the eddy diffusivity for momentum near the wall, is a function of the Reynolds number and the values for two-dimensional channel flow and circular pipe flow are different. It has a tendency to increase with the increase of the Reynolds number and approaches a constant value of $5{\cdot}23 \times 10^{-4}$ at very high Reynolds numbers. The value of $y_1{}^+$ and $y_2{}^+/H^+$ depend slightly on Reynolds number and have nearly constant values of about 26·3 and 0·23 respectively.

By using equations (28)–(30), the numerical values of κ_1 and κ_2 in equations (20) and (27) were computed to fit the experimental results of ε_H/ν by Mizushina *et al.* [3]. Thus, finally, the following equations were obtained.

$$y^+ \leqq y_H{}^+ \quad \phi_H = \frac{0{\cdot}0279\,(\varepsilon_M/\nu)^{\frac{1}{3}}\,Pr}{1 + 0{\cdot}228\,(\varepsilon_M/\nu)^{\frac{1}{3}}\,Pr^{\frac{1}{3}}} \qquad (31)$$

$$y^+ \geqq y_H{}^+ \quad \phi_H = \frac{0{\cdot}00681\,(\varepsilon_M/\nu)\,Pr}{1 + 0{\cdot}160\,(\varepsilon_M/\nu)^{\frac{1}{2}}\,Pr^{\frac{1}{3}}}; \qquad (32)$$

The values of $y_H{}^+$ at which the values of ϕ_H calculated by equations (31) and (32) are equal each other, are nearly constant at about 25 at large Prandtl and Reynolds numbers.

It is noted that the eddy diffusivity for heat in the region close to the wall is a function of the Reynolds number because the eddy diffusivity

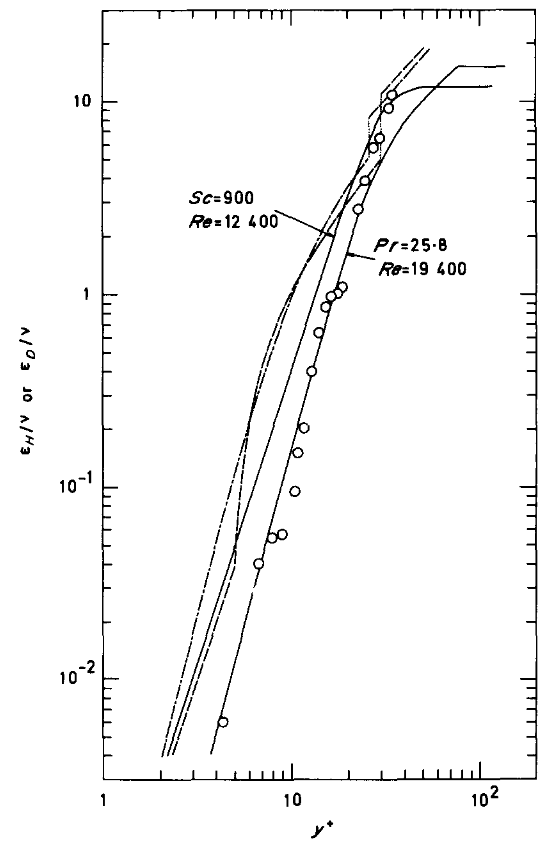

FIG. 2. Comparison of the calculated and measured values of eddy diffusivities for heat and mass; key, ○ experimental data at Pr = 25·8 and Re = 19 400, ——— calculated values, – – – – Lin *et al.* – · – · – · – Deissler.

for momentum in this region is a function of the Reynolds number as shown in Fig. 1.

If the mechanisms for eddy diffusion of heat and mass are assumed to be analogous, equations (31) and (32) are applicable to mass transfer by using ε_D and Sc instead of ε_H and Pr.

Comparison of the calculated eddy diffusivities with those measured at $Pr = 25{\cdot}8$ by Mizushina *et al.* [3], and at $Sc = 900$ by Lin *et al.*, is shown in Fig. 2. There is fairly good agreement between the calculated and experimental results.

Thus the Nusselt and Sherwood numbers can be calculated by substitution of the eddy diffusivities for heat or mass obtained by the above analysis into equations (9) and (10).

EXPERIMENTAL METHOD

The process chosen for this study was reduction of ferricyanide ions at a nickel cathode in the presence of a large excess of sodium and potassium hydroxide. This system has been used with good results by many previous investigators and offers a number of important advantages. The most significant advantage is that surface roughness can be kept very small compared with the dissolving wall method. This is particularly important at large Schmidt numbers because the surface roughness influences the mass transfer rate significantly in this case.

The experiments were performed in a rectangular duct of vinyl chloride, 5 by 50 mm cross section and 2 m long. The three nickel cathodes 398, 201 and 52 mm long and 20 mm wide, were mounted in series, flush with the upper surface in the center of the duct, the anode, 2 m long and 50 mm wide, being mounted on the lower surface of the duct. The cathodes were made narrower than the anode to ensure that the limiting current occurred at the cathodes rather than at the anode, and to eliminate any effects of flow disturbances in the corners of the duct.

The inlet length required to achieve the fully developed velocity profile at the cathode (mass transfer section) was about 100 times the equivalent diameter of the duct.

The measurements of mass transfer rates were made by a cathode 201 mm long, located downstream of a 398 mm long cathode. Thus the entry length for developing the concentration profile was $L^+ \approx 10^4$. Hence the measured mass transfer coefficient may be considered to be a fully developed one.

The electrolyte solution was recirculated through the duct by means of a vinyl chloride pump. To prevent the circulating fluid from becoming contaminated, vinyl chloride plastic valves and pipes were used throughout

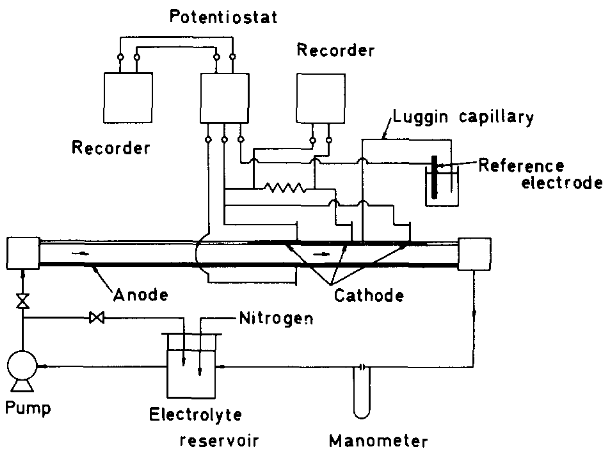

FIG. 3. Schematic diagram of the apparatus.

the system. The experimental apparatus is shown schematically in Fig. 3.

The solution used contained 0·001 ~ 0·01 M of $K_3Fe(CN)_6$ and $K_4Fe(CN)_6$ and 0·1 ~ 5·0 M of KOH and NaOH per liter. The concentration of ferricyanide ions at the cathode surface can be assumed to be zero at the limiting current, and the bulk concentration was measured with an iodometric titration.

The mass transfer coefficient is calculated by the following equation.

$$K = i/Fc_b. \tag{33}$$

The Reynolds and Schmidt numbers were varied from 3000 to 80 000 and 800–15 000, respectively. The flow rates were measured with a calibrated orifice in the pipe.

EXPERIMENTAL RESULTS

The experimental data is summarized in Table 1. The variations of K^+ with Re are plotted in Fig. 4, and compared with the prediction by equation (10) with the eddy diffusivity for mass presented in this analysis. The predicted values of K^+ have a tendency to decrease with decreasing Reynolds numbers because of the dependence of ε_M/ν on Re, and are in reasonable agreement with the measured values.

The variations of K^+ with Re are so small that the averaged values of the measured K^+ at various Reynolds numbers are plotted against Schmidt number in Fig. 5. For comparison with the predictions of the present analysis, of Deissler [2], and of Lin *et al.* [1], the experimental data of Harriott *et al.* [9] and Hubbard *et al.* [10] are also plotted in Fig. 5. The predictions of the authors fit the experimental results of the authors and Hubbard *et al.* quite well and are in good agreement with the prediction of Lin *et al.*, but in poor agreement with that of Deissler. The experimental results of Harriott *et al.* are slightly greater than the present prediction, probably because of the effect of the surface roughness.

The experimental results at Schmidt numbers of 15 100 and 782 are plotted as the Sherwood number vs. the Reynolds number in Fig. 6. and compared with the present prediction, the equation of Sieder and Tate [11], the analogy of Chilton and Colburn [12], and the prediction of Deissler. The experimental data shows that the Sherwood number varies with about 0·9 power of the Reynolds number at large Schmidt numbers, in reasonable agreement with the present prediction. It also appears from Fig. 6

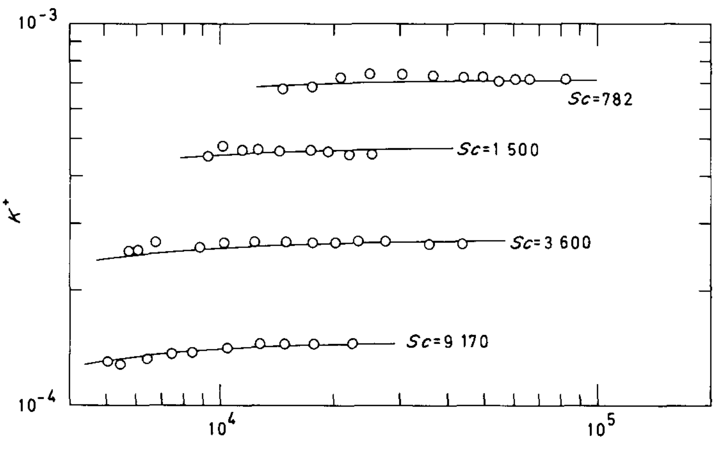

FIG. 4. Variation of K^+ with Reynolds number.

Table 1

Sc	*Re*	*Sh*	$K^{+} \times 10^{4}$
631	32,500	638	7·40
782	14,600	465	6·77
	17,500	552	6·85
	20,800	681	7·26
	24,900	810	7·39
	30,400	960	7·35
	36,800	1130	7·31
	44,200	1310	7·23
	49,900	1450	7·25
	54,900	1550	7·09
	60,600	1700	7·16
	66,200	1850	7·15
	82,400	2230	7·14
981	36,000	891	6·27
1200	22,000	669	5·08
1500	9310	399	4·49
	10,100	456	4·77
	11,400	490	4·65
	12,600	538	4·68
	14,300	594	4·62
	17,300	709	4·66
	19,300	770	4·61
	22,000	850	4·52
	25,400	960	4·56
2390	5630	310	3·42
	6080	317	3·27
	7320	374	3·28
	8600	444	3·38
	10,200	506	3·31
	13,200	631	3·30
	14,500	685	3·30
	15,900	748	3·33
	20,200	919	3·32
	26,800	1170	3·28
	35,600	1500	3·22
	41,000	1790	3·48
	44,800	1820	3·17
	57,400	2180	3·16
3600	5760	359	2·52
	6090	387	2·56
	6760	426	2·67
	8830	523	2·60
	10,200	623	2·68
	12,400	730	2·68
	15,000	859	2·68
	17,600	984	2·67
	20,200	1110	2·68
	23,200	1270	2·70
	27,500	1470	2·70
	36,000	1860	2·64
	44,000	2210	2·65
5480	4520	332	1·93
	5500	396	1·93
	6620	459	1·91
	7900	539	1·92
	9420	642	1·96
	10,900	728	1·95
	12,600	819	1·93
	13,400	883	1·99
	15,600	1020	1·99
	18,400	1170	1·98
	24,000	1490	2·00
9170	5050	411	1·30
	5450	432	1·27
	6460	514	1·31
	7470	613	1·37
	8440	683	1·37
	10,400	848	1·42
	12,700	1030	1·44
	14,700	1160	1·44
	17,700	1370	1·44
	22,500	1720	1·46
15,100	3570	377	0·980
	3800	403	0·990
	4600	478	0·994
	5280	535	0·988
	6200	616	0·987
	7200	723	1·02
	7950	785	1·01
	8960	884	1·03
	10,100	993	1·04
	12,300	1170	1·02
	14,000	1320	1·04
	15,500	1470	1·05

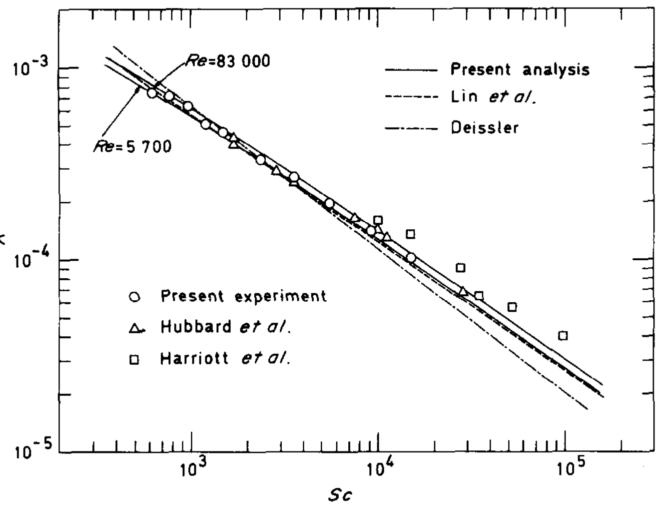

FIG. 5. Variation of K^+ with Schmidt number.

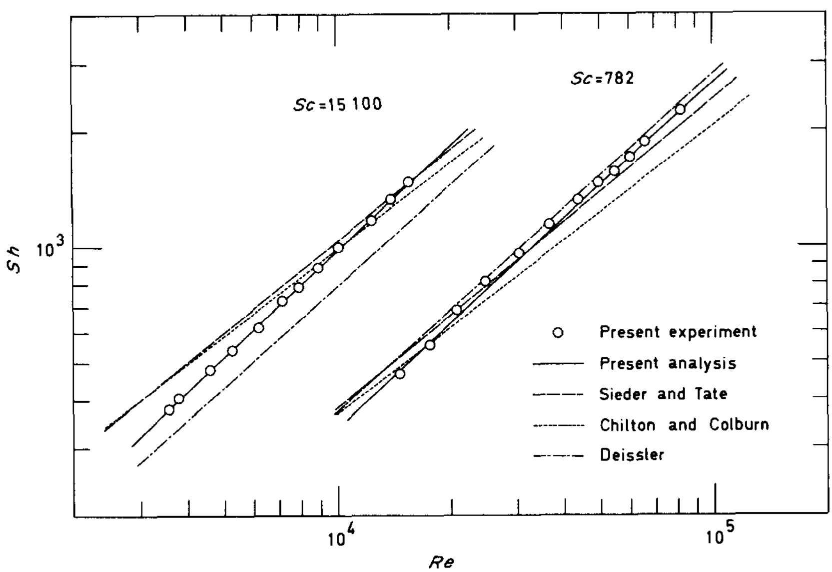

FIG. 6. Variation of Sherwood number with Reynolds number.

that the other three predictions apparently fail to represent the experimental results.

DISCUSSIONS

It is generally accepted that the exponent $1/n$ in the relation $Nu \propto Pr^{1/n}$ or $Sh \propto Sc^{1/n}$ follows from the fact that the eddy diffusivities near the wall vary with the n-th power of the distance from the wall. Hubbard *et al.* [10] concluded from their experimental results that the value of n was 3, but Son *et al.* [13] obtained the eddy diffusivity expression at $y^+ \to 0$ as $\varepsilon_D/\nu =$

$0{\cdot}00032\ (y^+)^4$ from their experiments on the dependence of Sc on Sh, and on the effect of the length of the transfer section on the rate of the mass transfer.

On the other hand, the eddy diffusivity of the present analysis shows that $\varepsilon_D/v \propto (y^+)^4$ at $y^+ \to 0$, but the calculated value of K^+ varies with $Sc^{-\frac{2}{3}}$, i.e. $Sh \propto Sc^{\frac{1}{3}}$ at large Schmidt numbers as shown in Fig. 5.

To discuss this problem further, the eddy diffusivity expressions of the present work may be simplified as follows.

Since the case considered is at large Prandtl or Schmidt numbers, only the equations (28) and (31), which are valid in the vicinity of the wall, are discussed here.

In the immediate vicinity of the wall, ε_M/v is very small. Hence from equations (23) and (31), the expression of the eddy diffusivity for heat is given by the following simple equation.

$$y^+ \leqq {y_B}^+ \qquad \varepsilon_H/v = 0{\cdot}0279\, A^{\frac{4}{3}}\, Pr\, (y^+)^4. \tag{34}$$

In the region where the magnitude of the product of Pr and ε_M/v is very large compared with unity, ε_H/v is given by

$$y^+ \geqq {y_B}^+ \qquad \varepsilon_H/v = A(y^+)^3. \tag{35}$$

y_B^+ is located at a boundary of two regions. where equations (34) and (35) are valid respectively, and is obtained by equating these two equations as follows,

$${y_B}^+ = 1/(0{\cdot}0279\, A^{\frac{1}{3}}\, Pr) \tag{36}$$

The value of ${y_B}^+$ is proportional to Pr^{-1}, and depends slightly on the Reynolds number because of the dependence of A on Re as shown in Fig. 1.

The thickness, δ^+, of the thermal boundary layer is defined simply as that which satisfies the following conditions:

$$\varepsilon_H/v\,\big|_{\text{at } y^+ = \delta^+} = 10^2/Pr. \tag{37}$$

When equation (37) is applied to equation (7), the value of the integrand of equation (7), i.e.

$$\frac{1}{1/Pr + \varepsilon_H/v},$$

becomes $Pr/(1 + 10^2) \doteqdot 0{\cdot}01\ Pr$ at $y^+ = \delta^+$, which is only 1 per cent of the value at $y^+ = 0$, i.e. Pr. Therefore, one can assume that

$$\int_0^\infty \frac{\mathrm{d}y^+}{1/Pr + \varepsilon_H/v} \doteqdot \int_0^{\delta^+} \frac{\mathrm{d}y^+}{1/Pr + \varepsilon_H/v} \tag{38}$$

and hence the value of T^* at $y^+ = \delta^+$ becomes nearly unity. Combining equation (37) with equations (34) or (35), one obtains the thickness of the boundary layer as

$$\delta^+ \leqq {y_B}^+ \qquad \delta^+ = 7{\cdot}74\, A^{-\frac{1}{3}}\, Pr^{-\frac{1}{2}} \tag{39}$$

$$\delta^+ \geqq {y_B}^+ \qquad \delta^+ = 4{\cdot}64\, A^{-\frac{1}{3}}\, Pr^{-\frac{1}{3}}. \tag{40}$$

In Fig. 7, ${y_B}^+$ and δ^+ are plotted against Prandtl number at $Re = 10^4$. As shown in Fig. 7, there are two regions where the eddy diffusivity varies with $(y^+)^4$ and $(y^+)^3$ in the thermal boundary layer at large Prandtl numbers. The eddy diffusivity for heat varies with $(y^+)^3$ in almost all parts of the boundary layer at $Pr > 10^3$. Hence the transfer coefficient is expressed approximately as

$$Pr > 10^3 \qquad h^+ \doteqdot 1 \Big/ \int_0^\infty \frac{\mathrm{d}y^+}{1/Pr + A(y^+)^3}$$

$$= 0{\cdot}827\, A^{\frac{1}{3}}\, Pr^{-\frac{2}{3}}. \tag{41}$$

Similarly, for mass transfer,

$$Sc > 10^3 \qquad K^+ = 0{\cdot}827\, A^{\frac{1}{3}}\, Sc^{-\frac{2}{3}}. \tag{42}$$

The conclusion of the discussion is that the relation $K^+ \propto (Sc)^{-\frac{2}{3}}$ at large Schmidt numbers does not indicate that $\varepsilon_D/v \propto (y^+)^3$ at $y^+ \to 0$, but that the eddy diffusivity varies with $(y^+)^3$ in the almost all parts of the boundary layer.

CONCLUSIONS

1. By using the revised expression for eddy diffusivity from the previous analysis, good agreement was obtained between the predicted and experimental results of mass transfer at Schmidt numbers between 800 and 15,000.
2. Both the predicted and experimental results

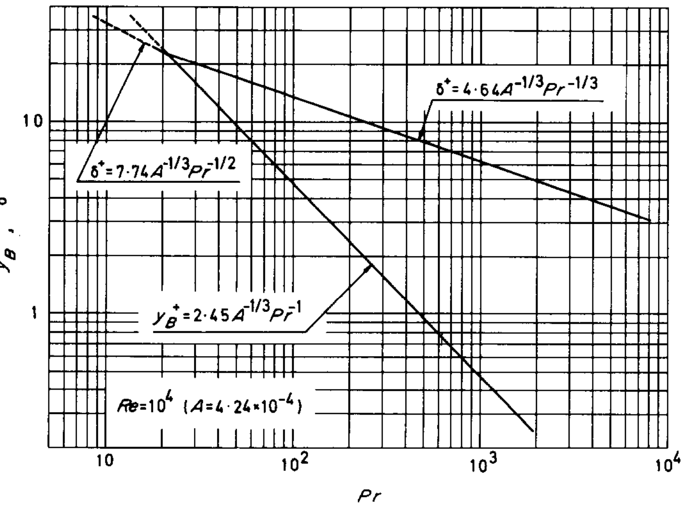

FIG. 7. Variation of δ^+ and $y_B{}^+$ with Prandtl number at $Re = 10^4$.

show that the Sherwood number varies with the $\frac{1}{3}$ power of the Schmidt number and about the 0·9 power of the Reynolds number at large Schmidt numbers.

ACKNOWLEDGEMENTS

The authors wish to express their thanks to the Japanese Ministry of Education and Hattori Hoko-kai for their financial support.

REFERENCES

1. C. S. LIN, R. W. MOULTON and G. L. PUTNAM, Mass transfer between solid wall and fluid streams, *Ind. Engng Chem.* **45**, 636 (1953).
2. R. G. DEISSLER, Analysis of turbulent heat transfer, mass transfer, and friction in smooth tubes at high Prandtl and Schmidt numbers, NACA Rep. 1210 (1955).
3. T. MIZUSHINA, R. ITO and F. OGINO, Eddy diffusivity distribution near the wall, presented at the Fourth International Heat Transfer Conference, FC2.8 (1970).
4. T. MIZUSHINA, R. ITO F. OGINO and H. MURAMOTO, Eddy diffusivities for heat in the region near the wall, *Mem. Fac. Engng Kyoto Univ.* **31**, 169 (1969).
5. W. E. RANZ and W. R. MARSHALL, Evaporation from drops. *Chem. Engng Prog.* **48**, 141 (1952).
6. J. O. HINZE, *Turbulence*, p. 285. McGraw-Hill, New York (1959).
7. T. MIZUSHINA and Y. KURIWAKI, Turbulent heat transfer in non-Newtonian fluids, *J. Engng Phys.* **12**, 152 (1967).
8. T. MIZUSHINA and F. OGINO, Eddy viscosity and universal velocity profile in turbulent flow in a straight pipe, *J. Chem. Engng Japan* **3**, 166 (1970).
9. P. HARRIOTT and R. M. HAMILTON, Solid–liquid mass transfer in turbulent pipe flow, *Chem. Engng Sci.* **20**, 1073 (1965).
10. D. W. HUBBARD and E. N. LIGHTFOOT, Correlation of heat and mass transfer data for high Schmidt and Reynolds numbers, *I/EC Fundamentals* **5**, 370 (1966).
11. E. N. SIEDER and G. E. TATE, Heat transfer and pressure drop of liquids in tubes, *Ind. Engng Chem.* **28**, 1429 (1936).
12. A. P. COLBURN, A method of correlating forced convection heat transfer data and a comparison with fluid friction, *Trans. A.I.Ch.E.* **29**, 174 (1933).
13. S. SON and T. J. HANRATTY, Limiting relation for the eddy diffusivity close to a wall, *A.I.Ch.E.Jl* **13**, 689 (1967).

TRANSFERTS THERMIQUE ET MASSIQUE PAR TURBULENCE ENTRE PAROI ET COURANTS FLUIDES POUR DES NOMBRES DE PRANDTL ET SCHMIDT GRANDS

Résumé—On a revu l'expression de la diffusion par turbulence dans une analyse antérieure. En utilisant cette expression corrigée, on a obtenu un bon accord entre les résultats prédits et ceux expérimentaux pour un transfert massique à des nombres de Schmidt compris entre 800 et 15 000.

Les résultats prédits et expérimentaux ont montré que le nombre de Sherwood varie selon la puissance $\frac{1}{3}$ du nombre de Schmidt et à peu près selon la puissance 0,9 du nombre de Reynolds quand $Sc = 800 \sim 15000$ et $Re = 3000 \sim 8000$

TURBULENTER WÄRME- UND STOFFÜBERGANG ZWISCHEN WAND UND STRÖMUNG BEI HOHEN PRANDTL- UND SCHMIDT-ZAHLEN

Zusammenfassung—Der Ansatz für den zusätzlichen Austauschkoeffizienten aus einer früheren Arbeit wurde verbessert. Mit diesem verbesserten Ansatz ergab sich eine gute Übereinstimmung zwischen den berechneten und den experimentellen Ergebnissen für den Stoffübergang bei Schmidt-Zahlen zwischen 800 und 15 000.

Die rechnerischen und die experimentellen Ergebnisse zeigen, dass sich die Sherwood-Zahl mit der Potenz $\frac{1}{3}$ der Schmidt-Zahl und der Potenz von etwa 0·9 der Reynolds-Zahl ändert für $Sc = 800 \ldots 15\,000$, und $Re = 3000 \ldots 80\,000$.

ТУРБУЛЕНТНЫЙ ПЕРЕНОС ТЕПЛА И МАССЫ МЕЖДУ СТЕНКОЙ И ПОТОКАМИ ЖИДКОСТИ ПРИ БОЛЬШИХ ЧИСЛАХ ПРАНДТЛЯ И ШИИДТА

Аннотация—Пересмотрено выражение вихревой диффузии, предложенное в предыдущей статье. С помощью нового выражения получено хорошее согоасие между расчётными и экспериментальными результатами для переноса массы при числах Шмидта, равный 800 и 15 000.

Расчётные и экспериментальные результаты показали, что число Шервуда изменяется как число Шмидта в степени $\frac{1}{3}$ и число Рейнольдса в степени 0,9 при $Sc = 800 \sim 15\,000$ и $Re = 3000 \sim 80\,000$.